Simplified model for inelastic acoustic phonon scattering of holes in Si and Ge

F. M. Bufler,[a] A. Schenk, and W. Fichtner
Institut für Integrierte Systeme, ETH Zürich, Gloriastrasse 35, CH-8092 Zürich, Switzerland

(Received 29 March 2001; accepted for publication 5 June 2001)

An averaging procedure is applied to inelastic acoustic–phonon scattering which leads to lattice-temperature-dependent constants for the phonon energy and the square of the phonon wave vector. The resulting scattering rate depends on energy only thus facilitating the search of after-scattering states in full-band Monte Carlo simulations. The model still accurately reproduces the velocity–field characteristics over a wide range of lattice temperatures, but in silicon the hot-hole tail of the energy distribution is strongly enhanced compared with the elastic equipartition approximation. © *2001 American Institute of Physics.* [DOI: 10.1063/1.1388597]

Full-band Monte Carlo simulation has been established as a powerful tool which allows one to incorporate sophisticated scattering models on a microscopic level.[1] However, the incorporation of complicated models often significantly increases the computational burden of the simulation and may also lead to additional uncertainties when, e.g., approximate discretization schemes are necessary for the inclusion of those models. Therefore, approximations are often being employed. One of the frequently used simplifications is the elastic equipartition approximation for acoustic–phonon scattering. Using this elastic model, it has been possible to reproduce the experimental data for the drift mobility or velocity of holes in Si or Ge both in the linear[2,3] and in the nonlinear[4,5] regime over a wide range of lattice temperatures to a high degree of accuracy. At the same time, the elastic model has the advantage of involving a scattering rate, which depends only on energy but not on the phonon wave vector, thus greatly facilitating the determination of the state after scattering during full-band Monte Carlo simulations. In addition, this model enables an exact computation of the ohmic drift mobility in terms of the microscopic relaxation time which requires only a one-dimensional integration over energy.[3,6] However, it has been recently found[7] that the elastic model in Si significantly underestimates the number of hot holes compared to an inelastic model which takes the acoustic–phonon dispersion into account and yields, after recalibration of the acoustic and optical coupling constants, a similar good agreement with experimental drift velocity data. It is therefore the aim of this article to develop a model which has the simple structure of the elastic model being advantageous for full-band Monte Carlo simulation, but involves on average essentially the same energy dissipation as the inelastic model and hence yields the correct hole energy distribution.

In general, the hole–phonon scattering rate is wave, vector-dependent and can be written in the form (see, e.g., Ref. 7)

$$S(\mathbf{k})=\sum_{\mathbf{k}'}\frac{\pi}{\rho\omega(q)}\Delta^2(q)\left(N_q+\frac{1}{2}\mp\frac{1}{2}\right)\times\frac{1}{V}\delta[\epsilon(\mathbf{k}')-\epsilon(\mathbf{k})\mp\hbar\omega(q)], \tag{1}$$

where we have suppressed the band indices and approximated the overlap integral as unity. ρ is the mass density, V the volume of the crystal, N_q the Bose–Einstein distribution, and the phonon wave vector $\mathbf{q}$ is determined by wave vector conservation. Upper and lower signs correspond to the absorption and emission of a phonon with energy $\hbar\omega(q)$, respectively, and the sum is over the final states $\mathbf{k}'$. In the case of optical phonons, both the coupling constant $\Delta(q)=D_tK$ and the phonon energy $\hbar\omega(q)=\hbar\omega_{\mathrm{opt}}\equiv k_B\theta_{\mathrm{opt}}$ are usually taken as constants introducing the equivalent phonon temperature θ_{opt}. The acoustic phonons are characterized in the isotropic approximation via $\Delta(q)=\mathcal{E}q$ and an analytical description of the acoustic–phonon dispersion $\omega(q)$. For the phonon dispersion, we adopt the formula $\hbar\omega(q)=\hbar(\nu_{\mathrm{SL}}q-c_Lq^2)$ of Ref. 7 which has the important property to reproduce the longitudinal sound velocity at $q=0$. The parameters in Si (Ge) are $\nu_{\mathrm{SL}}=9.0\times10^5$ cm/s (5.4×10^5 cm/s) and $c_L=2.0\times10^{-3}$ cm^2/s (1.2×10^{-3} cm^2/s).

In order to reduce the wave-vector-dependent acoustic scattering rate to an expression which depends only on energy, we replace both q^2 and $\hbar\omega(q)$ by constants instead of applying the elastic equipartition approximation. These constants are obtained by an averaging procedure in the following way. First, the modulus of the phonon wave vector, $q=\|\mathbf{k}'-\mathbf{k}\|$, is averaged over a sphere in the spirit of an isotropic, parabolic band structure with the result $q=4/3\,k$. Then the phonon energy, which is emitted or absorbed by a hole with a wave vector $\mathbf{k}$, is averaged with the equilibrium distribution function, i.e., the Maxwell–Boltzmann distribution. This leads to

$$k_B\theta_{\mathrm{ac}}\equiv\hbar\omega_{\mathrm{ac}}=\frac{\int d\epsilon\,\hbar\omega(\frac{4}{3}k(\epsilon))\mathcal{D}(\epsilon)e^{-\beta\epsilon}}{\int d\epsilon\,\mathcal{D}(\epsilon)e^{-\beta\epsilon}}, \tag{2}$$

with $\beta\equiv1/(k_BT)$, the density of states $\mathcal{D}(\epsilon)$ and $k(\epsilon)$

[a]Electronic mail: bufler@iis.ee.ethz.ch

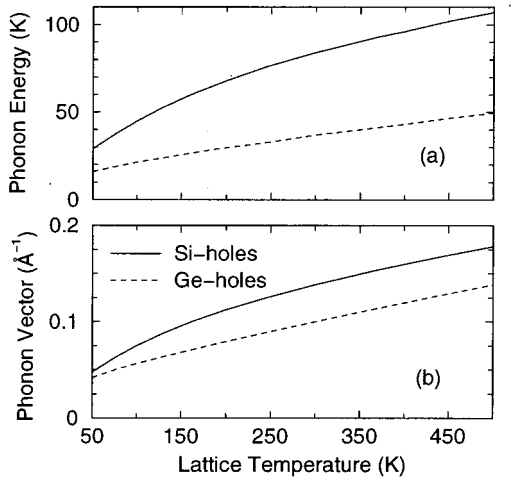

FIG. 1. Phonon energy (a), expressed in terms of the equivalent phonon temperature $\theta_{ac}=\langle\hbar\omega(q)\rangle/k_B$, and mean modulus of the phonon wave vector (b), defined via $\sqrt{\langle q^2\rangle}$, as a function of the lattice temperature are shown.

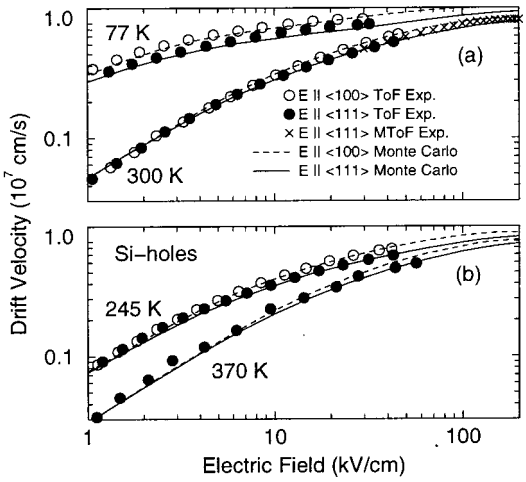

FIG. 2. Full-band Monte Carlo results for the velocity–field characteristics of holes in Si at different lattice temperatures in comparison with corresponding time-of-flight measurements (see Refs. 10 and 11) and microwave time-of-flight measurements (see Ref. 12) are shown.

$=\sqrt{2m(\epsilon)\epsilon}/\hbar$ where the effective mass $m(\epsilon)$ is taken to be the energy-dependent effective density-of-states mass.[8] Of course, the mean acoustic–phonon energy actually depends on the strength of the electric field. But at high fields, optical–phonon scattering is dominant so that inaccuracies of the acoustic–phonon model are less important in this regime. An analogous averaging procedure is used to compute the mean value of the squared phonon wave vector, $\langle q^2\rangle$. As a consequence of this approach, $\langle\hbar\omega(q)\rangle$ and $\langle q^2\rangle$ become lattice-temperature dependent which is shown in Figs. 1(a) and 1(b), respectively. The similar shapes of averaged phonon energy and squared wave vector indicate that the nonlinear contribution of the phonon dispersion is negligible. The smaller phonon energy of Ge in comparison to Si is due to the smaller sound velocity. Finally, we note that the underlying full-band structure of the three valence bands is calculated via the nonlocal empirical pseudopotential method[9] where in addition also the spin–orbit interaction is considered. An equidistant mesh in momentum space is employed with a mesh spacing of $1/96\times 2\pi/a$ with a being the lattice constant.

For the inelastic model, the acoustic and the optical coupling constant, $\mathcal{E}$ and D_tK, have been recalibrated in order to reproduce the experimental velocity–field characteristics. The resulting values are reported in Table I. In Figs. 2 and 3, the full-band Monte Carlo results for the velocity–field characteristics in Si and Ge, respectively, are compared with the corresponding time-of-flight measurements at different lattice temperatures. A similar good agreement as in the case of the elastic model[4,3] can be observed. Note, however, that the *optical* coupling constant resulting from the adjustment is smaller in the present model with inelastic acoustic phonons than in the model employing the elastic equipartition approximation (the acoustic constants cannot be directly compared because of the different definitions). This is the same tendency as for the elastic model of Ref. 5 compared to the corresponding inelastic model with the full acoustic–phonon dispersion in Ref. 7. The smaller optical coupling constant is the reason why the inelastic models lead to an enhanced high-energy tail of the energy distribution in silicon in comparison to their elastic counterparts. The energy distributions resulting from the elastic and the inelastic models are shown in Fig. 4. A similar enhancement of the number of hot holes in the inelastic model as in Ref. 7 can be seen. On the other hand, it is clear that the population of high-energetic hole states can be still increased by simply further lowering the optical coupling constant and readjusting the acoustic one in order to recover, e.g., the ohmic drift mobility at room tem-

TABLE I. Coupling constants and material parameters for Si and Ge are shown.

Material	$\mathcal{E}$ (eV)	D_tK (10^8 eV/cm)	θ_{opt} (K)	ρ (g/cm^3)	a (Å)
Si	5.03	8.7	731	2.33	5.43
Ge	3.5	7.0	430	5.32	5.65

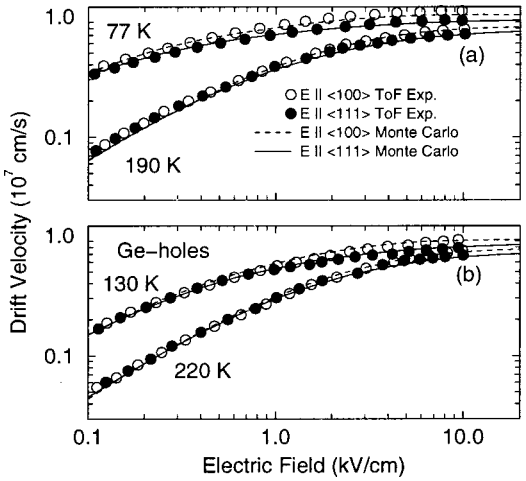

FIG. 3. Full-band Monte Carlo results for the velocity–field characteristics of holes in Ge at different lattice temperatures in comparison with corresponding time-of-flight measurements (see Ref. 13) are shown.

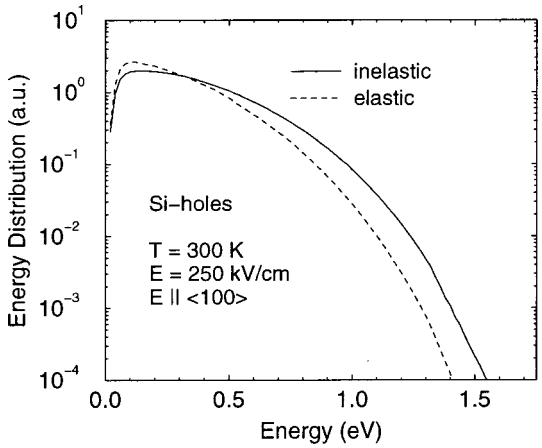

FIG. 4. Energy distribution as a function of the hole energy at 300 K for a field of 250 kV/cm in ⟨100⟩ direction is shown.

perature. However, this would in particular lead to both an underestimation of the experimental saturation velocity at room temperature[12] and an underestimation of the experimental velocities at 77 K and low fields[10] the latter being due to a too large acoustic coupling constant. These tendencies can indeed be observed in the literature.[14,15] In contrast, the energy distributions in Ge remain almost unchanged between the elastic and the inelastic models and are therefore not displayed. The reason is the much smaller acoustic–phonon energy in Ge which in turn requires only a smaller reduction of the optical coupling constant in order to reproduce the experimental velocity–field characteristics with the inelastic model. This explains why the elastic equipartition approximation works better in Ge than in Si.

In conclusion, a simplified model for inelastic acoustic–phonon scattering of holes in Si and Ge has been developed. The model has a scattering rate which depends only on energy thus facilitating the search of after-scattering states in full-band Monte Carlo simulations, accurately reproduces the experimental velocity–field characteristics over a wide range of lattice temperatures and recovers in Si the enhanced hot-hole tail of the energy distribution that results from a model involving a wave-vector-dependent acoustic–phonon dispersion.

This work was in part supported by the Kommission für Technologie und Innovation.

[1] *Monte Carlo Device Simulation: Full Band and Beyond*, edited by K. Hess (Kluwer, Dordrecht, 1991).
[2] M. V. Fischetti and S. E. Laux, J. Appl. Phys. **80**, 2234 (1996).
[3] F. M. Bufler and B. Meinerzhagen, J. Appl. Phys. **84**, 5597 (1998).
[4] F. M. Bufler, P. Graf, and B. Meinerzhagen, VLSI Design **8**, 41 (1998).
[5] B. Fischer and K. R. Hofmann, in *Proceedings of the International Conference on the Simulation of Semiconductor Processes and Devices, Leuven (Belgium), 1998*, edited by K. De Meyer and S. Biesemans (Springer, Berlin, 1998), p. 181.
[6] Y. Fu, K. J. Grahn, and M. Willander, IEEE Trans. Electron Devices **41**, 26 (1994).
[7] B. Fischer and K. R. Hofmann, Appl. Phys. Lett. **76**, 583 (2000).
[8] F. L. Madarasz, J. E. Lang, and P. M. Hemeger, J. Appl. Phys. **52**, 4646 (1981).
[9] M. M. Rieger and P. Vogl, Phys. Rev. B **48**, 14276 (1993).
[10] C. Canali, G. Ottaviani, and A. Alberigi-Quaranta, J. Phys. Chem. Solids **32**, 1707 (1971).
[11] C. Canali, G. Majni, R. Minder, and G. Ottaviani, IEEE Trans. Electron Devices **22**, 1045 (1975).
[12] P. M. Smith and J. Frey, Appl. Phys. Lett. **39**, 332 (1981).
[13] L. Reggiani, C. Canali, F. Nava, and G. Ottaviani, Phys. Rev. B **16**, 2781 (1977).
[14] M. V. Fischetti, N. Sano, S. E. Laux, and K. Natori, IEEE Journal of Technology Computer Aided Design (http://www.ieee.org/products/online/journal/tcad).
[15] Y. Kamakura, I. Kawashima, K. Deguchi, and K. Taniguchi, J. Appl. Phys. **88**, 5802 (2000).